

This document is confidential and is proprietary to the American Chemical Society and its authors. Do not copy or disclose without written permission. If you have received this item in error, notify the sender and delete all copies.

**New textures of chocolate are formed by polymorphic crystallization and template effects: velvet chocolate**

Journal:	<i>Crystal Growth &amp; Design</i>
Manuscript ID:	cg-2015-00660b.R1
Manuscript Type:	Article
Date Submitted by the Author:	n/a
Complete List of Authors:	Bayés-García, Laura; Universitat de Barcelona, Cristal·lografia, Mineralogia i Dipòsits Minerals Calvet, Teresa; Universitat de Barcelona, Cristal·lografia, Mineralogia i Dipòsits Minerals Cuevas-Diarte, Miquel; Universitat de Barcelona, Cristal·lografia, Mineralogia i Dipòsits Minerals Rovira, Enric; Enric Rovira S. L., Ueno, Satoru; Hiroshima University, Faculty of Applied Biological Science Sato, Kiyotaka; Hiroshima University, Faculty of Applied Biological Science

SCHOLARONE™  
Manuscripts

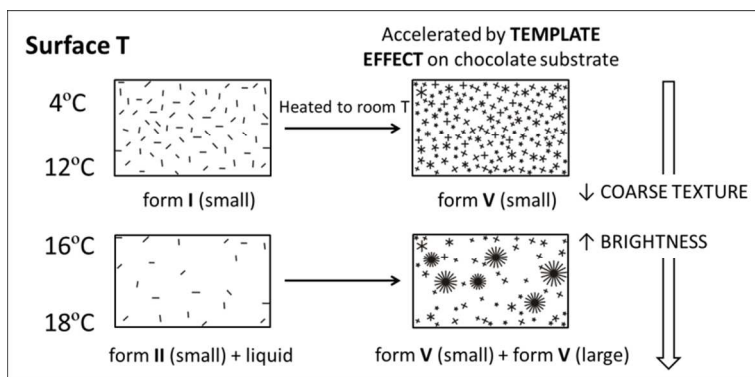
*New textures of chocolate are formed by polymorphic crystallization and template effects: velvet chocolate*

Laura Bayés-García<sup>\*a</sup>, Teresa Calvet<sup>a</sup>, Miquel Àngel Cuevas-Diarte<sup>a</sup>, Enric Rovira<sup>b</sup>, Satoru Ueno<sup>c</sup>, Kiyotaka Sato<sup>c</sup>

a. Departament de Cristal·lografia, Mineralogia i Dipòsits Minerals, Facultat de Geologia, Universitat de Barcelona, Martí i Franquès s/n, E-08028 Barcelona, Spain.

b. Enric Rovira S. L., Castellbell i el Vilar, Spain

c. Graduate School of Biosphere Science, Hiroshima University, Higashi-Hiroshima 739, Japan



New types of chocolate textures with a soft mouth-feel can be formed by controlling the crystallization and polymorphic transformation of cocoa butter (CB) with thermal treatment and template effects. A quick spray of molten chocolate liquor on chilled substrates (normally formed chocolate or metal) caused the crystallization of meta-stable forms of CB, which transformed to a stable form during subsequent heating processes. We characterized the domain sizes of  $\beta_V$  for the CB crystals in velvet chocolate, which were much smaller and exhibited a lower melting temperature and softer mouth feeling than those in normally tempered chocolate. Polymorphic crystallization and transformation of CB were in-situ monitored by X-ray diffraction by changing the temperatures of the substrates. The velvet effect was induced solely by decreasing the temperature of the substrates below 16°C, because crystallization of the metastable  $\gamma_I$  form and subsequent transformation to  $\beta_V$  of cocoa butter are prerequisites for forming velvet chocolate. The chocolate substrate was much more effective than the metal substrate in forming the velvet chocolate because of the template effect.

Laura Bayés-García ( [laurabayes@ub.edu](mailto:laurabayes@ub.edu) )

c/ Martí i Franquès s/n E-08028 Barcelona (Spain)

Tel. +34 93 4021350 / Fax. +34 93 402134

1  
2  
3  
4  
5  
6  
7  
8  
9  
10  
11  
12  
13  
14  
15  
16  
17  
18  
19  
20  
21  
22  
23  
24  
25  
26  
27  
28  
29  
30  
31  
32  
33  
34  
35  
36  
37  
38  
39  
40  
41  
42  
43  
44  
45  
46  
47  
48  
49  
50  
51  
52  
53  
54  
55  
56  
57  
58  
59  
60

# New textures of chocolate are formed by polymorphic crystallization and template effects: velvet chocolate

*Laura Bayés-García<sup>\*a</sup>, Teresa Calvet<sup>a</sup>, Miquel Àngel Cuevas-Diarte<sup>a</sup>, Enric Rovira<sup>b</sup>, Satoru Ueno<sup>c</sup>, and Kiyotaka Sato<sup>c</sup>*

<sup>a</sup>Departament de Cristal·lografia, Mineralogia i Dipòsits Minerals, Facultat de Geologia,  
Universitat de Barcelona, Martí i Franquès s/n, E-08028 Barcelona, Spain.

<sup>b</sup>Enric Rovira S. L., Castellbell i el Vilar, Spain

<sup>c</sup>Faculty of Applied Biological Science, Hiroshima University, Higashi-Hiroshima 739, Japan.

## ABSTRACT

We report new types of chocolate textures with a soft mouth-feel (velvet effect) formed by controlling the crystallization and polymorphic transformation of cocoa butter (CB) with thermal treatment and template effects. A quick spray of molten chocolate liquor on chilled substrates (normally formed chocolate or metal) caused the crystallization of meta-stable forms of CB, which transformed to a stable form during subsequent heating processes. Cryo-scanning electron microscopy and confocal interferometric scanning microscopy were employed to observe the surface structures of the velvet chocolate. We characterized the domain sizes of  $\beta_V$  for the CB

1  
2  
3 crystals in velvet chocolate, which were much smaller and exhibited a lower melting temperature  
4 and softer mouth feeling than those in normally tempered chocolate. Polymorphic crystallization  
5 and transformation of CB were in-situ monitored by X-ray diffraction by changing the  
6 temperatures of the substrates. It was obvious that the velvet effect was induced solely by  
7 decreasing the temperature of the substrates below 16°C, because crystallization of the  
8 metastable  $\gamma_I$  form and subsequent transformation to  $\beta_V$  of cocoa butter are prerequisites for  
9 forming velvet chocolate. The chocolate substrate was much more effective than the metal  
10 substrate in forming the velvet chocolate because of the template effect.  
11  
12  
13  
14  
15  
16  
17  
18  
19  
20  
21  
22  
23  
24  
25

## 26 INTRODUCTION

27  
28  
29  
30

31 Chocolate is made up of cocoa butter crystals as a continuous body, in which tiny particles of  
32 sugar, cacao mass and other ingredients are dispersed. Sharp melting and quick release of flavor  
33 and sweetness/bitterness are determined by the melting behavior of cocoa butter (CB) crystals.  
34 CB is composed of three main triacylglycerols (TAGs), 1,3-dipalmitoyl-2-oleoyl-glycerol (POP),  
35 1-3-distearoyl-2-oleoyl-glycerol (SOS), and rac-palmitoyl-stearoyl-2-oleoyl-glycerol (POS).  
36 Many studies have focused on the polymorphic behavior of CB<sup>1</sup> and its three main TAGs.<sup>2-6</sup>  
37 Cocoa butter exhibits six different polymorphic forms referred to as I through VI. Among them,  
38 form V is industrially promoted through tempering processes, as this polymorph provides the  
39 desired melting, textural, and mouth-feel characteristics of chocolate.<sup>7</sup>  
40  
41  
42  
43  
44  
45  
46  
47  
48  
49  
50  
51

52 Recently, we examined the influence of dynamic temperature variations on the polymorphic  
53 behavior of the principal TAGs of edible fats and oils.<sup>8-10</sup> The results indicated that, by tailoring  
54 specific cooling and heating rates, the polymorphic crystallization may be directed to obtain  
55  
56  
57  
58  
59  
60

1  
2  
3  
4  
5  
6  
7  
8  
9  
10  
11  
12  
13  
14  
15  
16  
17  
18  
19  
20  
21  
22  
23  
24  
25  
26  
27  
28  
29  
30  
31  
32  
33  
34  
35  
36  
37  
38  
39  
40  
41  
42  
43  
44  
45  
46  
47  
48  
49  
50  
51  
52  
53  
54  
55  
56  
57  
58  
59  
60

desired polymorphic forms with expected physicochemical properties for pharmaceutical, cosmetic, and food applications. We observed that more stable forms were directly obtained by decreasing the rate of cooling, whereas less stable forms predominated at high cooling rates. Thermal treatment may also modify crystal sizes and their distributions as reported by Acevedo et al.,<sup>11,12</sup> who observed nanometer-scale fat crystals (nanoplatelets) by using cryogenic transmission electron microscopy (cryo-TEM) and determined that fast cooling rates and the application of shear significantly decreased platelet length, width, and thickness. Further investigation was performed by Maleky et al.,<sup>13</sup> who quantified the effects of applying laminar shear on crystalline orientation and nanostructure triglyceride crystal networks of cocoa butter.

In this paper, we focus on the use of specific thermal treatments for developing new textures of chocolate with a soft mouth-feel, called the “velvet effect” (Fig. 1).

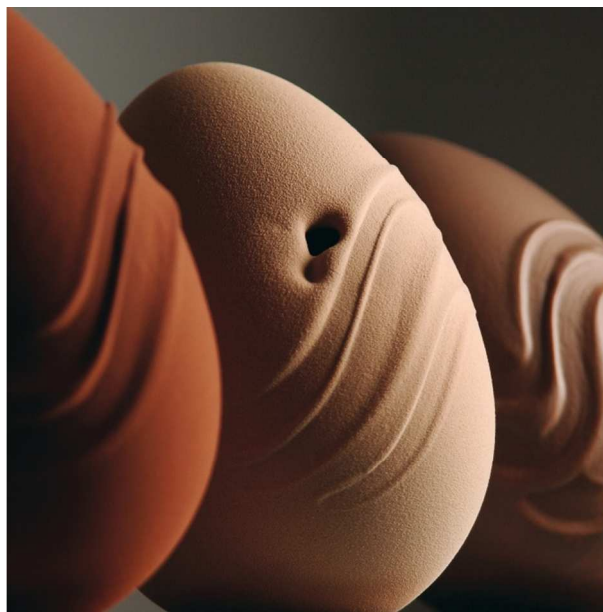


**Figure1.** Velvet effect appearance on chocolate eggs.

Mainly used in *gourmet* chocolate products, the velvet effect was first developed in 1963 by Catalan chocolatiers<sup>14</sup> and the use of this texture has spread internationally. However, no precise

1  
2  
3 work has been reported to clarify the formation of the velvet effect; the present study is the first  
4  
5 to do so.  
6  
7

8 The velvet effect is obtained when fluidized chocolate (a tempered mixture of chocolate and  
9  
10 cocoa butter) is sprayed on a cold chocolate surface. This process enables the formation of thin  
11  
12 layers of cocoa butter crystals with a lower melting point than that of normally tempered  
13  
14 chocolate, leading to the creation of a soft mouth-feel. Its name (velvet) is due to its soft but  
15  
16 rough appearance, obtained after cocoa butter crystallization.  
17  
18

19  
20 In this study, we characterized the velvet effect and monitored the polymorphic crystallization  
21  
22 and transformation that occur during rapid cooling and subsequent heating on the velvet effect  
23  
24 production. From the results obtained, the experimental conditions to obtain the desired  
25  
26 characteristics of an acceptable velvet effect could be optimized. The use of small droplets  
27  
28 obtained after spraying may accelerate the crystallization and transformation processes as it  
29  
30 offers very high cooling rates, both via large surface area-to-volume ratios and high rates of  
31  
32 convective heat and mass transfer, according to previous studies on spray freezing methods  
33  
34 applied to cocoa butter.<sup>15-17</sup> These researchers observed a polymorphic transformation similar to  
35  
36 those expected in a bulk mass of cocoa butter, but which occurred significantly faster in droplets.  
37  
38  
39

40  
41 We also studied the effects of different supercooling on polymorphic crystallization in velvet  
42  
43 preparation, and used two substrate materials (chocolate and metal) to analyze the template effect  
44  
45 caused by a chocolate surface, as template effects on lipid crystallization have been demonstrated  
46  
47 by previous work.<sup>18-21</sup>  
48  
49

## 50 51 52 53 EXPERIMENTAL SECTION 54 55 56 57 58 59 60

## Materials

Velvet chocolate and normal chocolate samples were prepared by Enric Rovira, master chocolatier (Enric Rovira S.L., Castellbell i el Vilar, Spain). Normal chocolate samples consisted of 70% cocoa chocolate (60% cocoa paste, 30% sugar, 10% cocoa butter and less than 1% soy lecithin).

## Sample preparation

To prepare the velvet chocolate, a mixture of 70% cocoa chocolate (Enric Rovira S.L.) and cocoa butter (Nederland S.A, Viladecans, Spain) was prepared in a ratio of 3:2 and tempered by completely melting the sample at 45°C, cooling it at 28°C and finally heating it at 32°C. The tempered mixture (fluidized chocolate) was sprayed on a cold surface (metal or chocolate at different temperatures) to cause rapid crystallization of the chocolate droplets. Spraying was performed using a Sagola 3300G Pro spraying gun with a 1.2mm nozzle. In this text, the term *fluidized chocolate* will be used to designate the tempered mixture of 70% cocoa chocolate and cocoa butter (3:2) which is sprayed to create velvet chocolate. This term will be used to distinguish the chocolate before spraying from *velvet chocolate*, which was obtained after spraying the fluidized chocolate on the cold surface.

## Differential scanning calorimetry

Differential scanning calorimetry (DSC) experiments were conducted at atmospheric pressure using a PerkinElmer Diamond. Samples were weighed into 50 $\mu$ l aluminum pans, and covers were sealed into place. The instrument was calibrated with reference to the enthalpy and the melting points of indium (melting temperature 156.6°C;  $\Delta H$  28.45J/g), and decane (melting

1  
2  
3 temperature  $-29.7^{\circ}\text{C}$ ;  $\Delta H$  202.1J/g) standards. An empty pan was used for reference. Dry  
4  
5 nitrogen was used as a purge gas in the DSC cell at  $20\text{cm}^3/\text{min}$ . Thermograms were analyzed  
6  
7 using Pyris Software to obtain the enthalpy (J/g, integration of the DSC signals) and peak top  $T$ ,  
8  
9  $T_{\text{onset}}$ , and  $T_{\text{end}}$  of the transitions ( $^{\circ}\text{C}$ , intersections of the baseline and the initial and final  
10  
11 tangents at the transition). Three independent measurements were made for each experiment  
12  
13 ( $n=3$ ). Random uncertainty was estimated with a 95% threshold of reliability using the Student's  
14  
15 method.  
16  
17  
18  
19  
20  
21

### 22 **Laboratory-scale X-ray diffraction**

23  
24 Laboratory-scale powder X-ray diffraction (XRD) allowed identifying, as a first stage, the  
25  
26 crystal forms present in velvet chocolate and comparing them with those in normal chocolate.  
27  
28 These initial measurements were performed using a PANalytical X'Pert Pro MPD powder  
29  
30 diffractometer equipped with a Hybrid Monochromator and PIXcel Detector. The equipment also  
31  
32 included an Oxford Cryostream Plus 220V (temperature 80 to 500K). This diffractometer  
33  
34 operated with Debye-Scherrer transmission. Samples were introduced in a 1mm-diameter  
35  
36 Lindemann glass capillary. The latter was rotated about its axis during the experiment to  
37  
38 minimize preferential orientations of the crystallites. The step size was  $0.026^{\circ}$  from  $1^{\circ}$  to  $40^{\circ} 2\theta$ ,  
39  
40 and the measuring time was 100 seconds per step.  
41  
42  
43  
44  
45

46  
47 Laboratory-scale powder XRD also enabled monitoring of the polymorphic transformations  
48  
49 that occurred during velvet formation. The fluidized chocolate sample was directly sprayed  
50  
51 either on a stainless steel metallic sample holder of maximum height of 4mm or on a chocolate  
52  
53 surface placed on the sample holder, at different temperatures ( $4^{\circ}\text{C}$ ,  $12^{\circ}\text{C}$ ,  $16^{\circ}\text{C}$  and  $18^{\circ}\text{C}$ ). Each  
54  
55 sample was subjected to XRD measurements taken during heating from chilled temperatures to  
56  
57  
58  
59  
60



1  
2  
3 room temperature (approximately 20°C). Temperatures were registered in a parallel experiment,  
4  
5 in identically simulated conditions. These XRD measurements were carried out using the same  
6  
7 powder diffractometer (PANalytical X'Pert Pro MPD) but using a convergent beam with a  
8  
9 focalizing mirror in reflection geometry. The step size was 0.026° from 1° to 30° 2θ, and the  
10  
11 measuring time was 10 seconds per step.  
12  
13  
14  
15  
16  
17

### 18 **Synchrotron radiation X-ray diffraction**

19  
20 Synchrotron radiation X-ray diffraction (SR-XRD) experiments were conducted on beamline  
21  
22 BL11-NCD at the synchrotron Alba (Cerdanyola del Vallès, Barcelona, Spain) at 12.4keV. The  
23  
24 sample-detector distance was 2.2m. X-ray scattering data were collected on a Quantum 210r  
25  
26 ADSC detector with a pixel size of 102.4x102.4μm<sup>2</sup> for the SAXD data and on a LX255-HS  
27  
28 Rayonix detector with a pixel size of 40x40mm<sup>2</sup> for the WAXD data. The exposure time was  
29  
30 20s. The temperature of the sample was controlled by a Linkam stage. SR-XRD patterns were  
31  
32 acquired while the sample was heated from 5 to 40°C at a controlled rate of 2°C/min. The sample  
33  
34 was placed in an aluminum sample cell with a Kapton film window. The q-axis calibration was  
35  
36 obtained by measuring silver behenate<sup>22</sup> for SAXD and Cr<sub>2</sub>O<sub>3</sub> for WAXD. The program pyFAI<sup>23</sup>  
37  
38 was used to integrate the 2D WAXD into the 1D data; the SAXD data were processed with in-  
39  
40 house software.  
41  
42  
43  
44  
45  
46  
47  
48

### 49 **Cryo-Scanning electron microscopy**

50  
51 Scanning electron microscopy (SEM) on frozen samples was performed with a JEOL JSM-  
52  
53 6510 scanning electron microscope equipped with an ALTO 1000 Cryotransfer System for SEM  
54  
55  
56  
57  
58  
59  
60

1  
2  
3 (Gatan) and an evacuation chamber. Samples were coated with gold-palladium prior to  
4  
5  
6 examination.

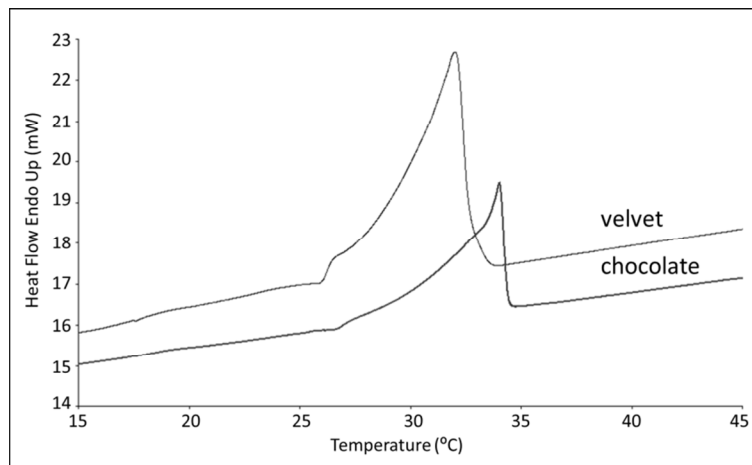
### 10 **Confocal Microscopy**

11  
12 A Leica DCM 3D (Leica Microsystems) confocal interferometric scanning microscope, with  
13  
14 10x, 20x, and 50x objectives, was used to capture images.  
15  
16  
17  
18  
19

## 20 RESULTS AND DISCUSSION

### 21 **Polymorphic and morphological characterization of velvet chocolate**

22  
23  
24 Figure 2 shows the DSC heating curves of normal chocolate and velvet chocolate, obtained  
25  
26 when the samples were heated from 5 to 50°C at a rate of 2°C/min.  
27  
28  
29  
30  
31



32  
33  
34  
35  
36  
37  
38  
39  
40  
41  
42  
43  
44  
45  
46  
47 **Figure 2.** DSC melting curves of velvet and normal chocolate when heated from 5 to 50°C at  
48  
49 2°C/min  
50  
51  
52  
53  
54  
55  
56  
57  
58  
59  
60

1  
2  
3  
4  
5  
6  
7  
8  
9  
10  
11  
12  
13  
14  
15  
16  
17  
18  
19  
20  
21  
22  
23  
24  
25  
26  
27  
28  
29  
30  
31  
32  
33  
34  
35  
36  
37  
38  
39  
40  
41  
42  
43  
44  
45  
46  
47  
48  
49  
50  
51  
52  
53  
54  
55  
56  
57  
58  
59  
60

The melting peak of velvet chocolate occurred at a significantly lower temperature than that of normal chocolate. The onset, peak top, and end temperatures of the normal chocolate DSC peak were  $27.9 \pm 0.4^\circ\text{C}$ ,  $34.1 \pm 0.3^\circ\text{C}$ , and  $34.5 \pm 0.4^\circ\text{C}$ , respectively, whereas the velvet DSC melting peak exhibited a  $T_{\text{onset}}$  of  $26.8 \pm 0.4^\circ\text{C}$ , peak top temperature of  $32.1 \pm 0.3^\circ\text{C}$ , and  $T_{\text{end}}$  of  $32.7 \pm 0.6^\circ\text{C}$ .

Figure 3 presents laboratory-scale XRD patterns of the polymorphic forms of the CB crystals present in the velvet samples taken at room temperature.

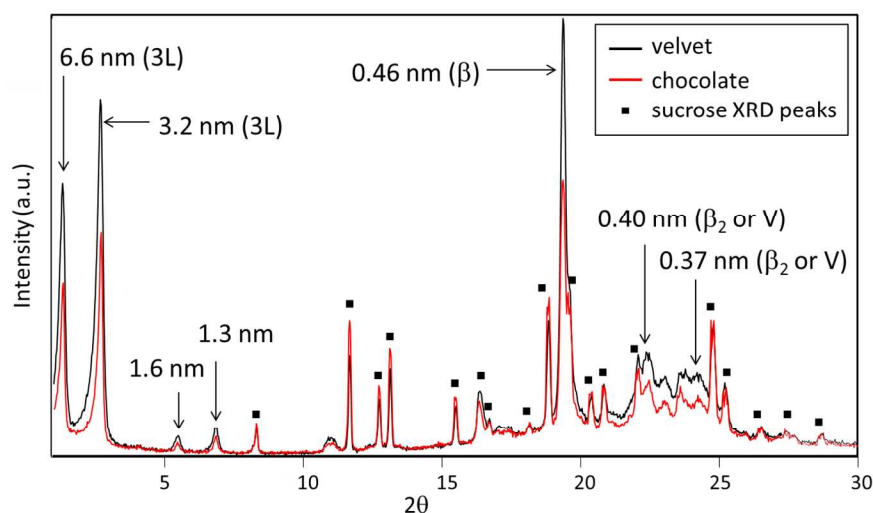


**Figure 3.** Laboratory-scale XRD of velvet and normal chocolate samples taken at room temperature.

The results showed identical XRD patterns for velvet and normal chocolates, revealing the presence of form V, with triple chain length structure XRD peaks at 6.6 and 3.2nm, and typical short spacing values of 0.46, 0.40, and 0.37nm. XRD peaks of the sucrose present in the samples are indicated by the symbol ■. Thus, the difference in the melting points of velvet and normal

chocolates was not due to the difference in the polymorphic forms of CB. However, the peaks of small-angle XRD patterns of the velvet chocolate were broader than those of normal chocolate. Broader diffraction peaks are related to smaller crystal size in a direction perpendicular to the scattering planes, through the Scherrer equation,<sup>24</sup> as discussed below.

The melting of form V CB crystals in the velvet chocolate was confirmed by SR-XRD with simultaneous SAXD/WAXD measurements (Fig. 4). The SR-XRD patterns were acquired while the sample was heated from 5 to 40°C at a controlled rate of 2°C/min, following the thermal treatment carried out by DSC.

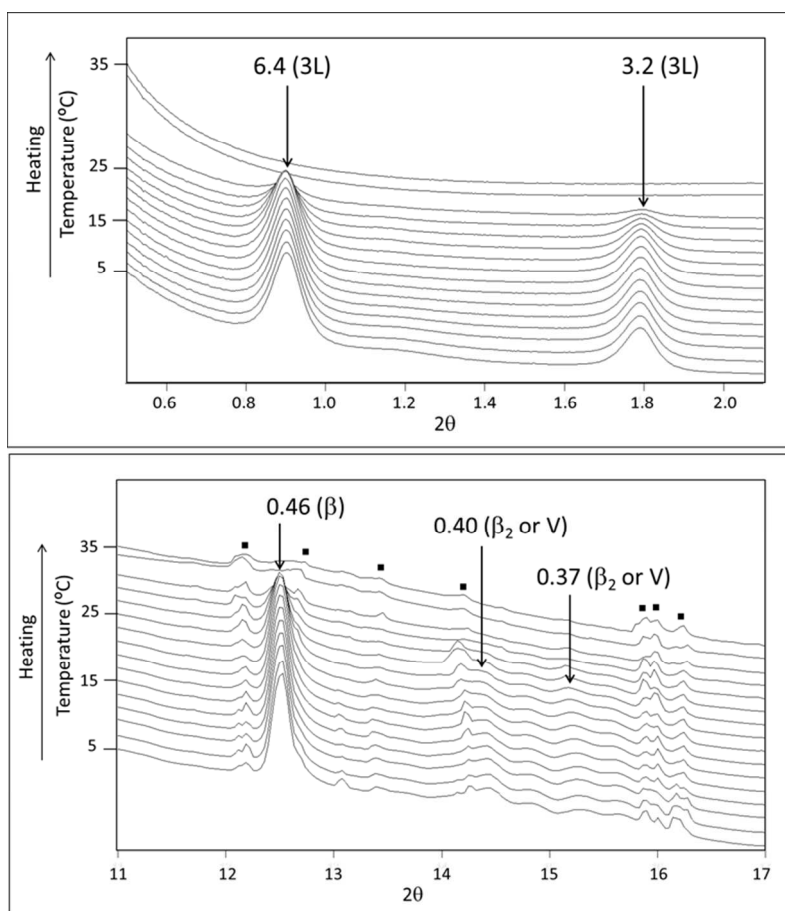


**Figure 4.** SR-SAXD (up) and SR-WAXD (bottom) patterns of velvet chocolate when heated from 5°C to 40°C at 2°C/min.

1  
2  
3 The SAXD pattern revealed the presence of triple chain length structure peaks at 6.4 and  
4 3.2nm, whereas form V cocoa butter in the velvet chocolate was confirmed by typical SR-  
5 WAXD peaks. Form V XRD peaks disappeared at around 33°C due to melting of the cocoa  
6 butter crystals. The remaining SR-WAXD peaks were due to sucrose present in the sample  
7 (noted by the symbol ■) after the CB melting.  
8  
9

10  
11  
12  
13  
14  
15  
16  
17  
18  
19  
20  
21  
22  
23  
24  
25  
26  
27  
28  
29  
30  
31  
32  
33  
34  
35  
36  
37  
38  
39  
40  
41  
42  
43  
44  
45  
46  
47  
48  
49  
50  
51  
52  
53  
54  
55  
56  
57  
58  
59  
60

Cryo-scanning electron microscopy was also carried out in order to observe the velvet particle morphology. As depicted in Fig. 5, the velvet morphology consisted of aggregates of round particles of around 30-50 $\mu$ m diameter. The round morphology was due to the rapid cooling of the sprayed chocolate droplets on the cold surface.

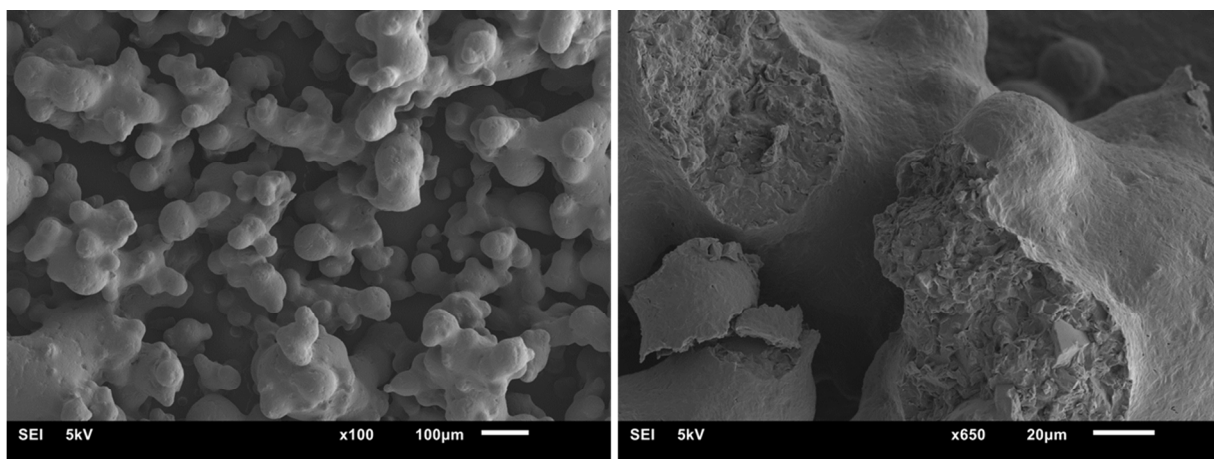


**Figure 5.** Cryo-SEM images of velvet chocolate

In Fig. 5 (right), one may also notice the presence of cocoa butter microstructure with embedded sugar crystals inside the aggregates of round particles.

Additional information on the morphological characterization of velvet was provided by confocal interferometric scanning microscopy. With this technique, the profile (peak-valley

heights) of one layer of round-particle aggregates could be determined (Fig. 6). Thus, several confocal microscopy images were taken in different areas of the velvet chocolate sample, and peak-to-valley distances were included in the range from 80 to 200 $\mu\text{m}$ .

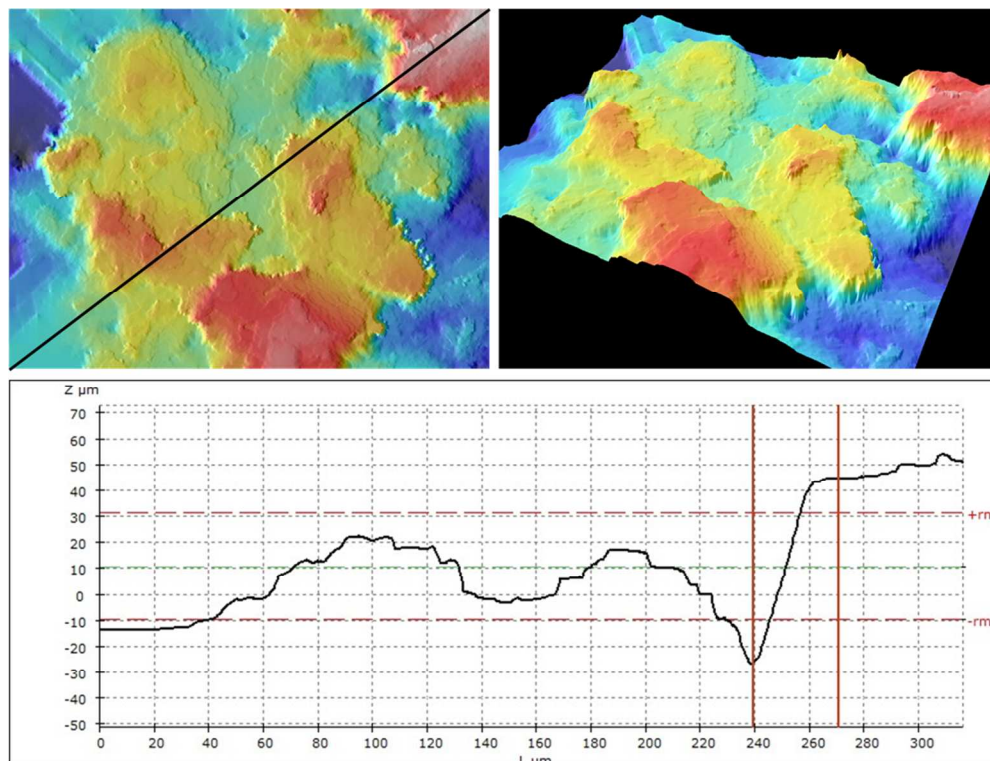


**Figure 6.** Confocal interferometric scanning microscopy image in 2D (top-left) and 3D (top-right), and profile of peak-to-valley heights (bottom). The profile depicted corresponds to the direction noted by a line in the 2D image.

### Scherrer analysis

The Scherrer equation<sup>24</sup> was used to estimate the thickness of the primary cocoa butter crystals.

$$\tau = (K \cdot \lambda) / (\beta \cdot \cos \theta)$$

1  
2  
3 Here,  $\lambda$  is the wavelength (nm),  $\theta$  is the Bragg angle at 2/3 of the height of the peak under  
4 study (rad),  $\beta$  describes the line broadening at half of the maximum intensity of the peak  
5 (FWHM, rad), and  $K$  is a dimensionless shape factor, that is close to unity and is related to the  
6 crystallite shape and to the way in which  $\beta$  and the thickness are defined. Scherrer analysis is an  
7 approximate method that assumes monodisperse crystals. This equation is only valid for  
8 crystallites smaller than 100nm and, as broadening increases with the diffraction angle, may be  
9 used for peaks in the small-angle region.  
10  
11  
12  
13  
14  
15  
16  
17  
18  
19

20 We used a  $K$  value of 0.9 to estimate the crystal thickness. This calculation is valid for well-  
21 defined, isolated, and symmetric peaks, so we selected the (005) diffraction peak (corresponding  
22 to a long-spacing value of 12.9Å, see Fig. 3) for the two samples. The FWHM of the peaks was  
23 estimated to be  $0.21^\circ 2\theta$  for the velvet chocolate sample and  $0.16^\circ 2\theta$  for normal chocolate,  
24 giving estimated crystal sizes of 37nm and 52nm, respectively.  
25  
26  
27  
28  
29  
30  
31

32 Considering this estimated crystal size domain and the lamellar size, determined from the long-  
33 spacing value of the (001) reflection (65.7Å), we estimated the number of lamellae in a crystal  
34 domain, as described elsewhere.<sup>25</sup> The results obtained are presented in Table 1.  
35  
36  
37  
38  
39  
40  
41

42 **Table 1.** Scherrer analysis data: crystal domain size and number of lamellae in a crystal domain  
43 in velvet and normal chocolate  
44  
45

	Velvet	Normal chocolate
Crystal domain (Å)	370	520
Lamellar size (long spacing value, Å)	65.7	65.7
Number of lamellae in a crystal domain	5.6	7.9

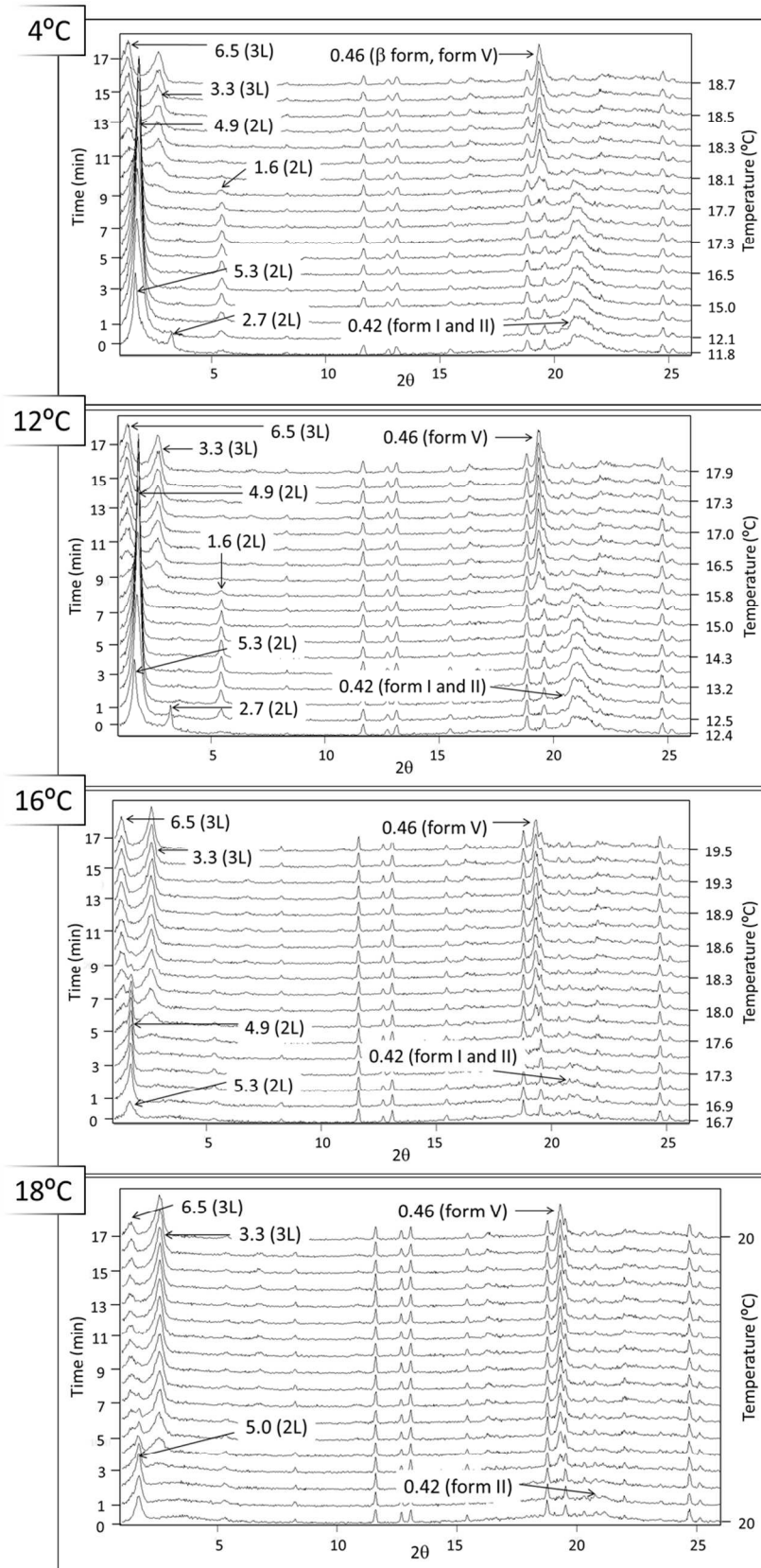
1  
2  
3 The difference in the XRD peak width between the velvet and normal chocolates indicated a  
4 smaller crystal size domain in the velvet, which could be estimated by Scherrer analysis. This  
5 smaller crystal size may be the reason for the lower melting temperature of form V velvet  
6 compared to that of normal chocolate.  
7  
8  
9  
10  
11

### 12 13 14 15 **Laboratory-scale XRD monitoring of chocolate velvet formation** 16

17 Laboratory-scale XRD experiments were performed to monitor the formation of form V soon  
18 after spraying. Molten chocolate was sprayed on metal and chocolate surfaces at different  
19 temperatures in order to analyze the influence of the temperature and the kind of substrate  
20 (normal chocolate or metal) on the crystallization and transformation of CB crystals after  
21 spraying. Furthermore, as already stated, by following this procedure, the experimental  
22 conditions to obtain an acceptable velvet effect could also be determined.  
23  
24  
25  
26  
27  
28  
29  
30

31 Figure 7 presents laboratory-scale XRD data obtained when fluidized chocolate was sprayed  
32 on a metal surface at 4°C, 12°C, 16°C, and 18°C and heated to room temperature.  
33  
34  
35  
36  
37  
38  
39  
40  
41  
42  
43  
44  
45  
46  
47  
48  
49  
50  
51  
52  
53  
54  
55  
56  
57  
58  
59  
60



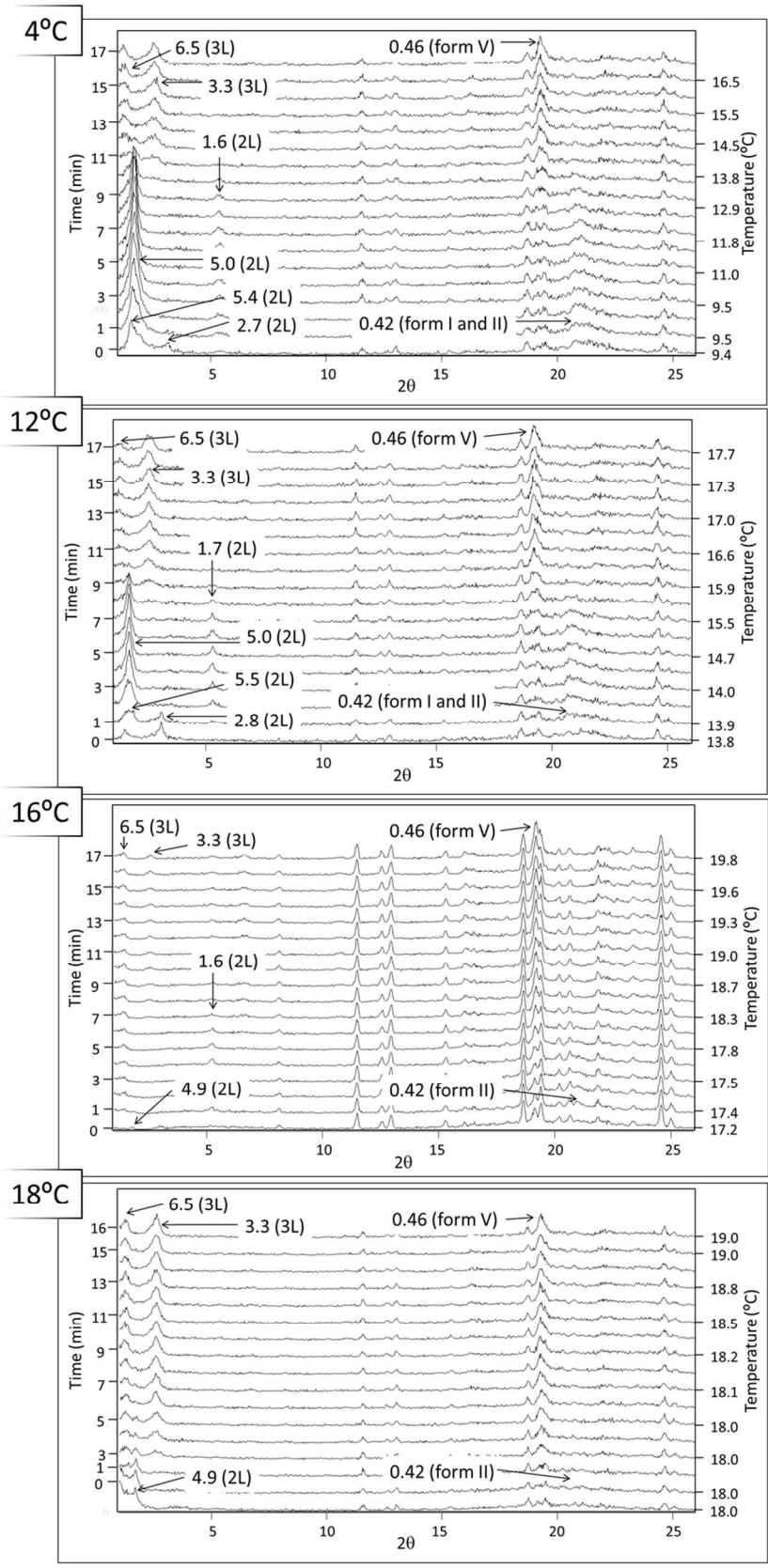


1  
2  
3 **Figure 7.** Laboratory-scale XRD patterns obtained when fluidized chocolate was sprayed on  
4 metal substrate at 4, 12, 16 and 18°C, and heated to room temperature.  
5  
6  
7  
8  
9  
10

11        Soon after the fluidized chocolate was sprayed on the metal surface at 4°C, initial form I  
12 developed and rapidly transformed to form II. A broad XRD peak at 0.42nm identifies both  
13 forms I and II. However, small-angle diffraction peaks became more suitable for distinguishing  
14 the two polymorphic forms, as there was no overlap with sucrose peaks at that  $2\theta$  range. Thus,  
15 peaks with long-spacing values of 5.3nm and 2.7nm correspond to the double chain length  
16 structure (2L) of form I, whereas the main 2L peak of form II appeared at 4.9nm. Ten minutes  
17 after spraying (when the sample reached a temperature around 18°C), form V developed, as a  
18 typical main XRD peak of  $\beta$  form appeared at 0.46nm, accompanied by triple chain length  
19 diffraction peaks (3L) at 6.5 and 3.3nm. The form II  $\rightarrow$  form V transformation ended at minute  
20 13, in which the peak at 4.9nm disappeared.  
21  
22  
23  
24  
25  
26  
27  
28  
29  
30  
31  
32  
33  
34

35        The same sequence of transformation was observed when the metal temperature was 12°C and  
36 16°C. However, in both results, the duration for the transformation to form V became shorter  
37 than that with a metal temperature of 4°C. Specifically, the presence of form V was detected nine  
38 and (five) minutes after spraying when the metal temperature was 12°C (16°C). Slightly different  
39 behavior was observed when the metal temperature was 18°C. In this case, form I did not  
40 develop, as droplets directly crystallized into form II, and form V was detected just three minutes  
41 after spraying. By comparing XRD data obtained at different temperatures of the metal surface,  
42 one may easily note that the intensity of the XRD peaks, especially small-angle diffraction peaks,  
43 of forms I and II decreased as the initial temperature of the metal increased from 4°C to 18°C.  
44  
45  
46  
47  
48  
49  
50  
51  
52  
53  
54  
55  
56  
57  
58  
59  
60

1  
2  
3 The same experiments were carried out by spraying fluidized chocolate on a chocolate  
4 substrate (see laboratory-scale XRD patterns in Fig. 8).  
5  
6  
7  
8  
9  
10  
11  
12  
13  
14  
15  
16  
17  
18  
19  
20  
21  
22  
23  
24  
25  
26  
27  
28  
29  
30  
31  
32  
33  
34  
35  
36  
37  
38  
39  
40  
41  
42  
43  
44  
45  
46  
47  
48  
49  
50  
51  
52  
53  
54  
55  
56  
57  
58  
59  
60



1  
2  
3  
4  
5  
6  
7  
8  
9  
10  
11  
12  
13  
14  
15  
16  
17  
18  
19  
20  
21  
22  
23  
24  
25  
26  
27  
28  
29  
30  
31  
32  
33  
34  
35  
36  
37  
38  
39  
40  
41  
42  
43  
44  
45  
46  
47  
48  
49  
50  
51  
52  
53  
54  
55  
56  
57  
58  
59  
60

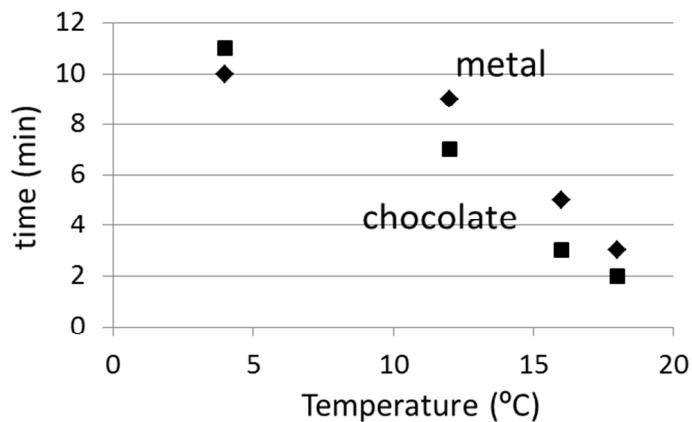
1  
2  
3 **Figure 8.** Laboratory-scale XRD patterns obtained when fluidized chocolate was sprayed on  
4 chocolate substrate at 4, 12, 16 and 18°C, and heated to room temperature.  
5  
6  
7  
8  
9

10  
11 The first occurring metastable form was form I with 2L structure peaks at 5.4nm and 2.7nm  
12 and a main short-spacing value of 0.42nm when the temperature of chocolate surface was 4°C,  
13 quite similar to those using the metal substrate. This form quickly transformed into form II (with  
14 a 5.0nm main long-spacing peak) and, 11 minutes after spraying (at a temperature of 18.0°C), the  
15 typical XRD peak of form V cocoa butter was detected at 0.46nm. 3L structure peaks at 6.5nm  
16 and 3.3nm also indicated form V occurrence. Compared to the metal substrate, the duration for  
17 the development of forms I and II became shorter as the initial temperature of the chocolate  
18 surface before spraying increased. Hence, form V appeared seven, three and two minutes after  
19 spraying when the chocolate surface temperature was 12°C, 16°C, and 18°C, respectively.  
20  
21 However, unlike the spraying experiment on a metal surface at 16°C, when velvet was grown on  
22 a chocolate surface at the same temperature, form II was directly crystallized from the melt  
23 without the development of form I.  
24  
25  
26  
27  
28  
29  
30  
31  
32  
33  
34  
35  
36  
37  
38

39 Table 2 summarizes the time and temperature at which form V developed when sprayed  
40 crystallization of chocolate was performed on both metal and chocolate substrates at 4°C, 12°C,  
41 16°C, and 18°C. The initially formed metastable forms for each condition are also specified.  
42  
43 Figure 9 indicates the durations necessary to complete the transformation from form II to form V  
44 CB crystals at the two surfaces with different substrate temperatures.  
45  
46  
47  
48  
49  
50  
51  
52  
53  
54  
55  
56  
57  
58  
59  
60

**Table 2.** Time and temperature for form V occurrence for experiments on metal and chocolate substrates at 4, 12, 16 and 18°C. Metastable forms obtained soon after spraying are also specified at each condition.

		Metal	Chocolate
4°C	t (min)	10	11
	T (°C)	18.0	13.8
	Metastable forms	I + II	I + II
12°C	t (min)	9	7
	T (°C)	15.8	15.5
	Metastable forms	I + II	I + II
16°C	t (min)	5	3
	T (°C)	17.6	17.5
	Metastable forms	I + II	II
18°C	t (min)	3	2
	T (°C)	20	18
	Metastable forms	II	II



1  
2  
3 **Figure 9.** Duration for form V formation of CB crystals on metal and chocolate substrates at the  
4 different temperatures.  
5  
6  
7  
8  
9  
10

11 From these results, it is clear that form V cocoa butter developed more rapidly on the chocolate  
12 substrate than on the metal substrate. This fact may be related to the template effect on the rate of  
13 form II → form V transformation by the chocolate substrate.  
14  
15  
16

17 However, when the spraying was performed at 4°C, form V developed on the metal substrate  
18 one minute earlier than on the chocolate substrate. This may be explained by considering the  
19 different thermal conductivities of metal and chocolate. For all of the experiments, the velvet  
20 temperature was registered soon after spraying and was monitored until the end of the XRD  
21 measurements. Just after spraying chocolate on a surface to create velvet, the temperature  
22 increased due to the hot sprayed chocolate. More importantly, the temperature increased  
23 especially if the surface temperature was considerably below room temperature, as in the case of  
24 a surface temperature of 4°C. By interpreting the data in Table 2, soon after spraying on the  
25 metal and chocolate substrates at 4°C, the temperature of the velvet was considerably higher  
26 when sprayed on the metal (11.8°C) than when sprayed on the chocolate (9.4°C), due to the  
27 higher thermal conductivity of metal. The initial temperatures for the two different materials  
28 were therefore not comparable, and due to the higher thermal conductivity of metal, its velvet  
29 chocolate temperature reached room temperature more quickly. Although form V appeared one  
30 minute later on the chocolate substrate, it occurred at 13.8°C (see Table 2), whereas form V was  
31 first detected at 18.0°C when metal was used. Despite this one minute difference, the template  
32 effect may also exist in this case, as a difference of 4.2°C was registered between the velvet  
33  
34  
35  
36  
37  
38  
39  
40  
41  
42  
43  
44  
45  
46  
47  
48  
49  
50  
51  
52  
53  
54  
55  
56  
57  
58  
59  
60

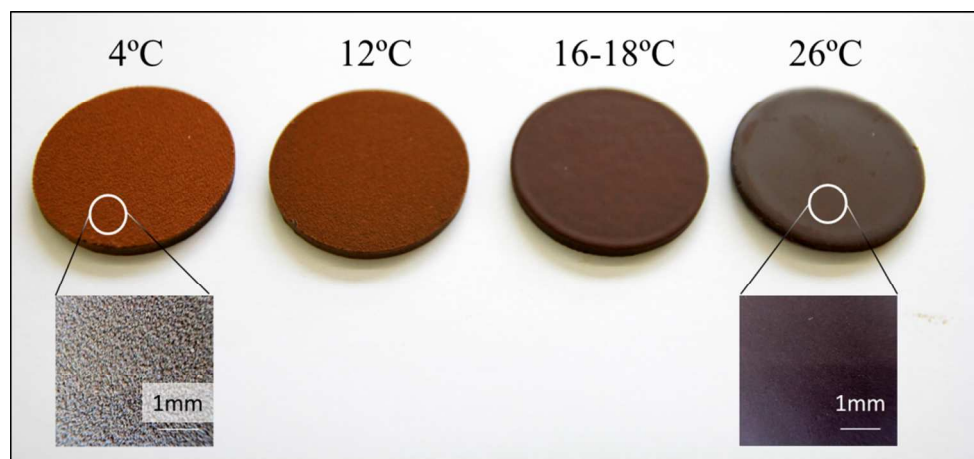
1  
2  
3 chocolates grown on the metal and chocolate substrates, and higher temperatures may accelerate  
4  
5 the polymorphic transformation.  
6  
7

8 When the temperatures of the metal and chocolate surfaces were closer to room temperature  
9  
10 (12°C, 16°C and 18°C), no significant differences in the initial temperatures after spraying were  
11  
12 observed when chocolate or metal were used as substrate material, as seen in Table 2.  
13  
14

15 The template effect caused by the chocolate surface was also confirmed by the metastable  
16  
17 forms observed at the first stage of crystallization. For both metal and chocolate substrates, forms  
18  
19 I and II were detected for surface temperatures of 4°C and 12°C. However, with an initial  
20  
21 temperature of 16°C, forms I and II were present when metal was used, whereas only the more  
22  
23 stable form II was present when the chocolate substrate was sprayed.  
24  
25  
26

27 In any case, the small crystallized droplets caused by spraying may result in a large contact  
28  
29 surface, which may accelerate polymorphic crystallization and transformation, as previous  
30  
31 studies reported.<sup>15-17</sup>  
32  
33

34 Figure 10 depicts the velvet grown on the chocolate surface at 4°C, 12°C, 16-18°C, and 26°C,  
35  
36 several hours after spraying, so after polymorphic crystallization and transformation ceased.  
37  
38 Enlarged images were taken for velvet chocolate grown at 4°C and 26°C.  
39  
40  
41  
42  
43





1  
2  
3 **Figure 10.** Appearance of velvet grown on chocolate surface at 4, 12, 16-18 and 26°C.  
4  
5

6  
7 The appearance of the velvet was the same at 16°C and 18°C. Velvet was also grown on  
8  
9 chocolate at above room temperature (26°C). One may appreciate the typical coarse texture of  
10  
11 velvet at 4°C and 12°C. However, the fluidized chocolate sprayed on chocolate became softer  
12  
13 and brighter as the substrate temperature increased, yielding a texture highly similar to that of  
14  
15 normally tempered chocolate when the temperature was 26°C, which cannot be considered a  
16  
17 velvet effect. Also, the color of the velvet chocolate became darker as the chocolate surface  
18  
19 temperature increased.  
20  
21

22  
23 One may be able to define a critical temperature above which velvet cannot be properly  
24  
25 formed. At 16°C and above, the coarse texture of velvet is lost, so lower temperatures (preferably  
26  
27 4-12°C) must be used in order to obtain the desired mouth-feel of velvet. The XRD data obtained  
28  
29 during velvet formation at different temperatures (Figs. 7 and 8) indicated that the amount of  
30  
31 metastable forms I and II decreased as the substrate temperature increased. Thus, the  
32  
33 development of metastable forms may be the key factor for developing an acceptable velvet  
34  
35 effect.  
36  
37

38  
39 Figure 11 summarizes the results obtained when velvet was grown at different temperatures  
40  
41 (different supercooling).  
42  
43  
44  
45  
46  
47  
48  
49  
50  
51  
52  
53  
54  
55  
56  
57  
58  
59  
60

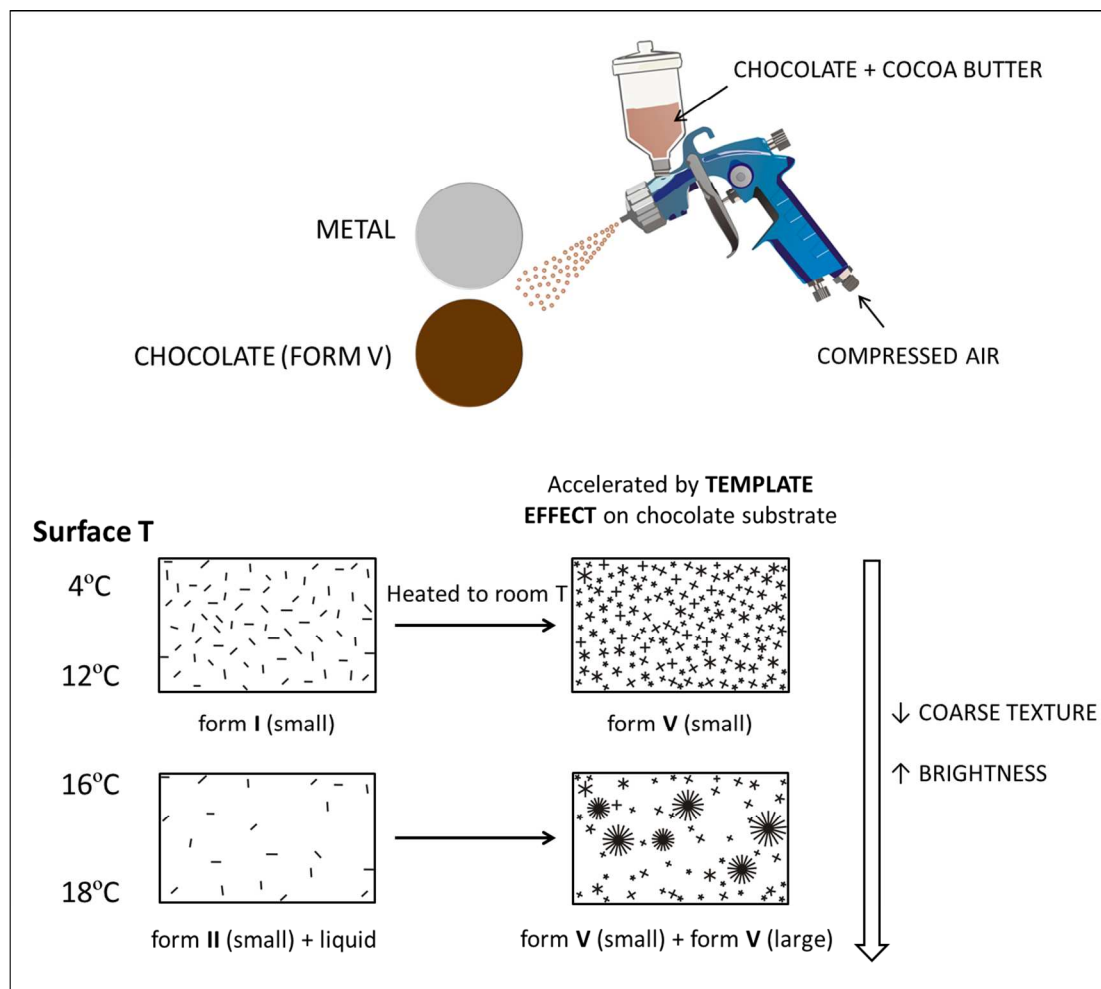


**Figure 11.** Models for describing the microstructure of velvet chocolate when grown at different surface temperatures on chocolate substrate.

When using a substrate temperature of 4°C or 12°C, metastable form I with small crystals developed and transformed to form V (through form II) as the sample reached room temperature. Form I then transformed to form V in the solid state, maintaining their small crystals. The thus-formed small form V crystals of CB in the velvet chocolate had a lower melting point than normally tempered chocolate, in which the form V crystals are larger. However, when fluidized chocolate was sprayed on the substrates at higher temperatures, the more stable form II was

1  
2  
3 directly crystallized. Under such conditions, not all of the cocoa butter may have crystallized, so  
4  
5 form II coexisted with some amount of liquid, as XRD data demonstrated with the increase in  
6  
7 background when the substrate temperature increased (Figs. 7 and 8). Hence, the initially  
8  
9 developed form II may have transformed to form V while keeping small crystals, whereas the  
10  
11 liquid present in the sample may have crystallized into form V with its larger crystals (more  
12  
13 similar to normally tempered chocolate). The formation of larger crystals of form V may be  
14  
15 responsible for the softer and brighter texture observed when higher substrate temperatures, such  
16  
17 as 26°C, were used (Fig. 10).  
18  
19  
20  
21  
22  
23

## 24 CONCLUSIONS

25  
26  
27 The present study demonstrated that thermal treatments may be applied to developing new  
28  
29 chocolate textures, such as the velvet effect. This texture was defined as form V of cocoa butter,  
30  
31 with a smaller crystal domain size, which led to a lower melting point and, therefore, to a soft  
32  
33 mouth-feeling. By monitoring the velvet effect formation using laboratory-scale X-ray  
34  
35 diffraction, we identified the first occurrence of form I, and subsequent polymorphic  
36  
37 transformations I → II → V, upon heating. Precursor forms I and II may be key factors for  
38  
39 obtaining form V, with smaller crystal size domains compared to normally tempered chocolate.  
40  
41 This difference in crystal size domains was revealed by Scherrer analysis. These polymorphic  
42  
43 transformations were accelerated by the template effect when chocolate substrate was used. The  
44  
45 appearance of the velvet (e.g. roughness, color, brightness) largely depended on the supercooling  
46  
47 (temperature of the substrate). Thus, the surface became coarser and duller as the supercooling  
48  
49 increased. When the supercooling decreased (for substrate temperatures from 16 to 26°C), the  
50  
51  
52  
53  
54  
55  
56  
57  
58  
59  
60

1  
2  
3 appearance of the velvet became more similar to normally-tempered chocolate (softer and  
4  
5 brighter), as shown in Figure 10.  
6  
7

8  
9  
10 AUTHOR INFORMATION

11  
12 **Corresponding Author**

13  
14 Phone: +34 93 402 13 50. Fax: +34 93 402 13 40. E-mail: [laurabayes@ub.edu](mailto:laurabayes@ub.edu)  
15  
16

17  
18 ACKNOWLEDGEMENT

19  
20  
21 Funding from the Alba synchrotron facility for performing SR-XRD experiments is gratefully  
22  
23 acknowledged. SR-XRD experiments were conducted with the approval of the Alba Scientific  
24  
25 Advisory Committee (proposal 2011120041). The authors wish to thank Dr. Marc Malfois,  
26  
27 responsible for BL11-NCD at Alba, for his help. The authors also acknowledge the Generalitat  
28  
29 de Catalunya through the Grup Consolidat 2014SGR1208.  
30  
31  
32

33  
34  
35 REFERENCES

- 36  
37  
38  
39 1. Timms, R. E. *Confectionary Fats Handbook*; The Oily Press: Bridgwater, 2003.  
40  
41  
42 2. Sato, K.; Arishima, T.; Wang, Z. H.; Ojima, W. K.; Sagi, N.; Mori, H. *J. Am. Oil Chem. Soc.*  
43  
44 **1989**, 66, 664-674.  
45  
46  
47 3. Koyano, T.; Hachiya, I.; Arishimo, T.; Sato, K.; Sagi, N. *J. Am. Oil Chem. Soc.* **1989**, 66,  
48  
49 675-679.  
50  
51  
52  
53 4. Miura, S.; Konishi, H. *Eur. J. Lipid Sci. Technol.* **2001**, 103, 804-809.  
54  
55  
56 5. Arishima, T.; Sagi, N.; Mori, H.; Sato, K. *J. Am. Oil Chem. Soc.* **1991**, 68, 710-715.  
57  
58  
59  
60

- 1  
2  
3 6. Rousset, P.; Rappaz, M. *J. Am. Oil Chem. Soc.* **1997**, 74, 1693-1697.  
4  
5  
6 7. Cocoa Butter and Related Compounds. Garti, N.; Widlak, N. R., Eds. AOCS Press: Urbana,  
7  
8 2012.  
9  
10  
11 8. Bayés-García, L.; Calvet, T.; Cuevas-Diarte, M. A.; Ueno, S.; Sato, K. *CrystEngComm*  
12 **2011**, 13, 3592-3599.  
13  
14  
15 9. Bayés-García, L.; Calvet, T.; Cuevas-Diarte, M. A.; Ueno, S.; Sato, K. *CrystEngComm*  
16 **2013**, 15, 302-314.  
17  
18  
19 10. Bayés-García, L.; Calvet, T.; Cuevas-Diarte, M. A.; Ueno, S.; Sato, K. *J. Phys. Chem. B*  
20 **2013**, 117, 9170-9181.  
21  
22  
23 11. Acevedo, N. C.; Marangoni, A. G. *Cryst. Growth Des.* **2010**, 10, 3327–3333.  
24  
25  
26 12. Acevedo, N. C.; Marangoni, A. G. *Cryst. Growth Des.* **2010**, 10, 3334–3339.  
27  
28  
29 13. Maleky, F.; Smith, A. K.; Marangoni, A. *Cryst. Growth Des.* **2011**, 11, 2335-2345.  
30  
31  
32 14. Escribá Serra, A. *Felices Pascuas... en chocolate*. Barcelona, 1967.  
33  
34  
35 15. Gwie, C. G.; Griffiths, R. J.; Cooney, D. T.; Johns, M. L.; Wilson, D. I. *J. Am. Oil Chem.*  
36 *Soc.* **2006**, 83, 1053-1062.  
37  
38  
39 16. Pore, M.; Seah, H. H.; Glover, J. W. H.; Holmes, D. J.; Johns, M. L.; Wilson, D. I.;  
40 Moggridge, G. D. *J. Am. Oil Chem. Soc.* **2009**, 86, 215-225.  
41  
42  
43 17. Talhat, A. M.; Lister, V. Y.; Moggridge, G. D.; Rasburn, J. R.; Wilson D. I. *J. Food Eng.*  
44 **2015**, 156, 67-83.  
45  
46  
47  
48  
49  
50  
51  
52  
53  
54  
55  
56  
57  
58  
59  
60

- 1  
2  
3 18. Smith, K.; Bhaggan, K.; Talbot, G.; van Malssen, K. *J. Am. Oil Chem. Soc.* **2011**, 88, 1085-  
4 1101.  
5  
6  
7  
8  
9 19. Sato, K.; Bayés-García, L.; Calvet, T.; Cuevas-Diarte, M. A.; Ueno, S., *Eur. J. Lipid Sci.*  
10 *Technol.* **2013**, 115, 1224-1238.  
11  
12  
13  
14 20. Verstringe, S.; Dewettinck, K.; Ueno, S.; Sato, K. *Cryst. Growth Des.* **2014**, 14, 5219-  
15 5226.  
16  
17  
18  
19  
20 21. Shimamura, K.; Ueno, S.; Miyamoto, Y.; Sato, K. *Cryst. Growth Des.* **2013**, 13, 4746-  
21 4754.  
22  
23  
24  
25  
26 22. Huang, T. C.; Toraya, H.; Blanton, T. N.; Wu, Y. *J. Appl. Cryst.* **1993**, 26, 180-184.  
27  
28  
29 23. Kieffer, J.; Karkoulis, D. *J. Phys.: Conf. Ser.* **2013**, 425, 202012.  
30  
31  
32 24. Scherrer, P. *Gött. Nachr.* **1918**, 2, 98-100.  
33  
34  
35 25. Peyronel, F.; Campos, R. In *Structure-Function Analysis of Edible Fats*. Marangoni, A. G.,  
36 Ed. AOCS Press: Urbana, 2012.  
37  
38  
39  
40  
41  
42  
43  
44  
45  
46  
47  
48  
49  
50  
51  
52  
53  
54  
55  
56  
57  
58  
59  
60

FOR TABLE OF CONTENTS USE ONLY

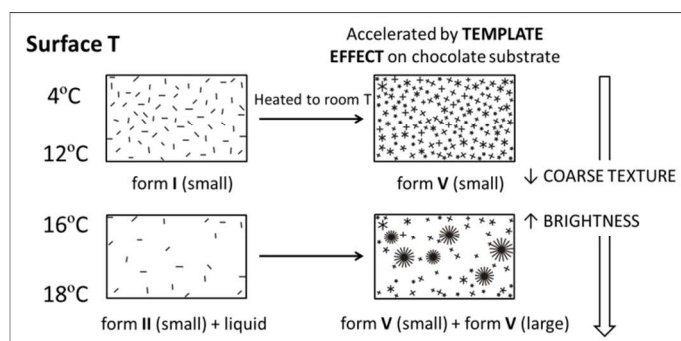
New textures of chocolate are formed by polymorphic crystallization and template effects: velvet chocolate

Laura Bayés-García\*<sup>a</sup>, Teresa Calvet<sup>a</sup>, Miquel Àngel Cuevas-Diarte<sup>a</sup>, Enric Rovira<sup>b</sup>, Satoru Ueno<sup>c</sup>, Kiyotaka Sato<sup>c</sup>

a. Departament de Cristal·lografia, Mineralogia i Dipòsits Minerals, Facultat de Geologia, Universitat de Barcelona, Martí i Franquès s/n, E-08028 Barcelona, Spain.

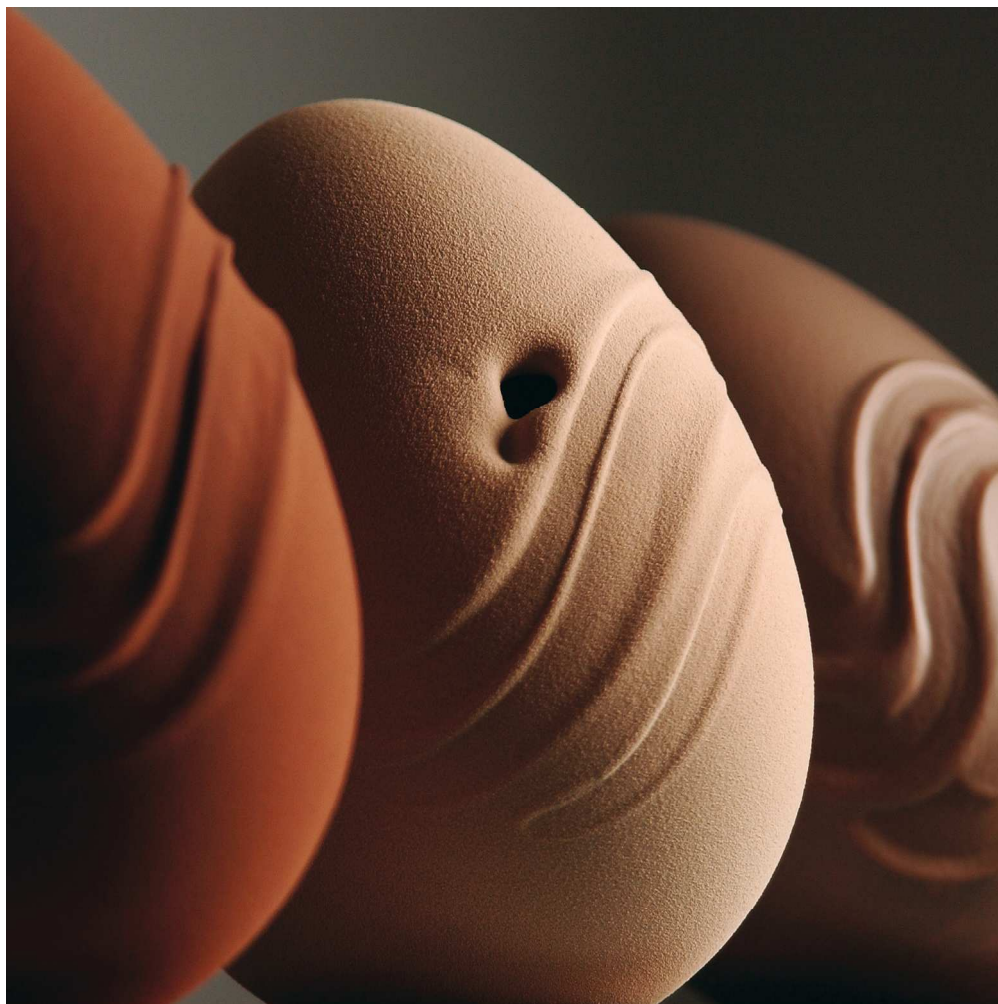
b. Enric Rovira S. L., Castellbell i el Vilar, Spain

c. Graduate School of Biosphere Science, Hiroshima University, Higashi-Hiroshima 739, Japan



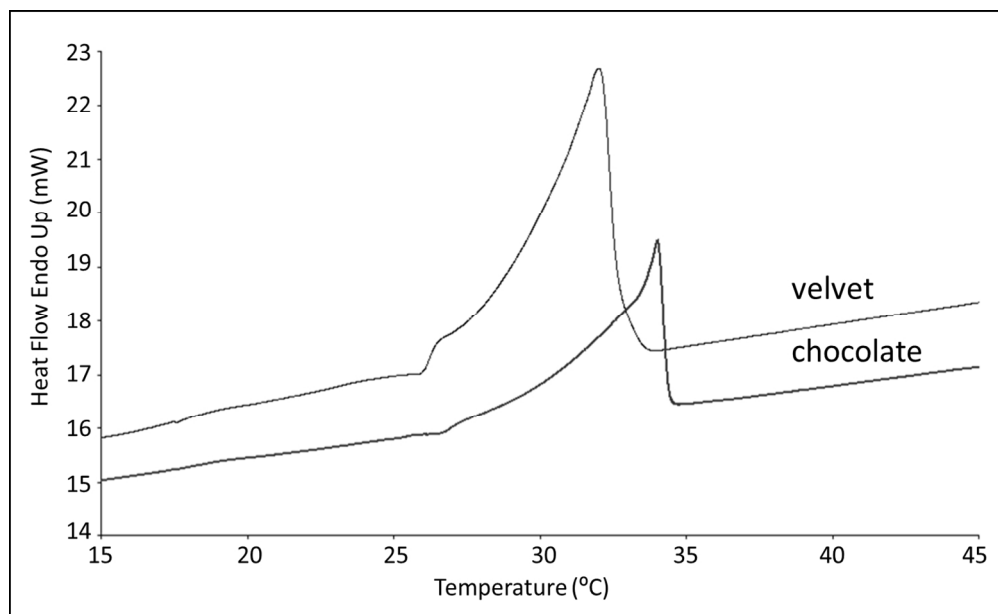
New types of chocolate textures with a soft mouth-feel can be formed by controlling the crystallization and polymorphic transformation of cocoa butter with thermal treatment and template effects.

1  
2  
3  
4  
5  
6  
7  
8  
9  
10  
11  
12  
13  
14  
15  
16  
17  
18  
19  
20  
21  
22  
23  
24  
25  
26  
27  
28  
29  
30  
31  
32  
33  
34  
35  
36  
37  
38  
39  
40  
41  
42  
43  
44  
45  
46  
47  
48  
49  
50  
51  
52  
53  
54  
55  
56  
57  
58  
59  
60

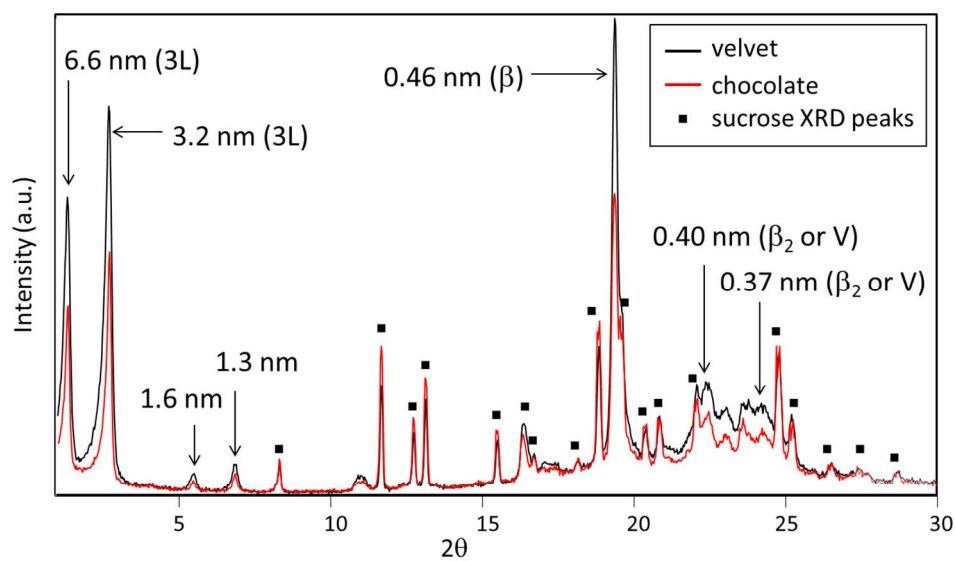


Velvet effect appearance on chocolate eggs.  
161x161mm (300 x 300 DPI)

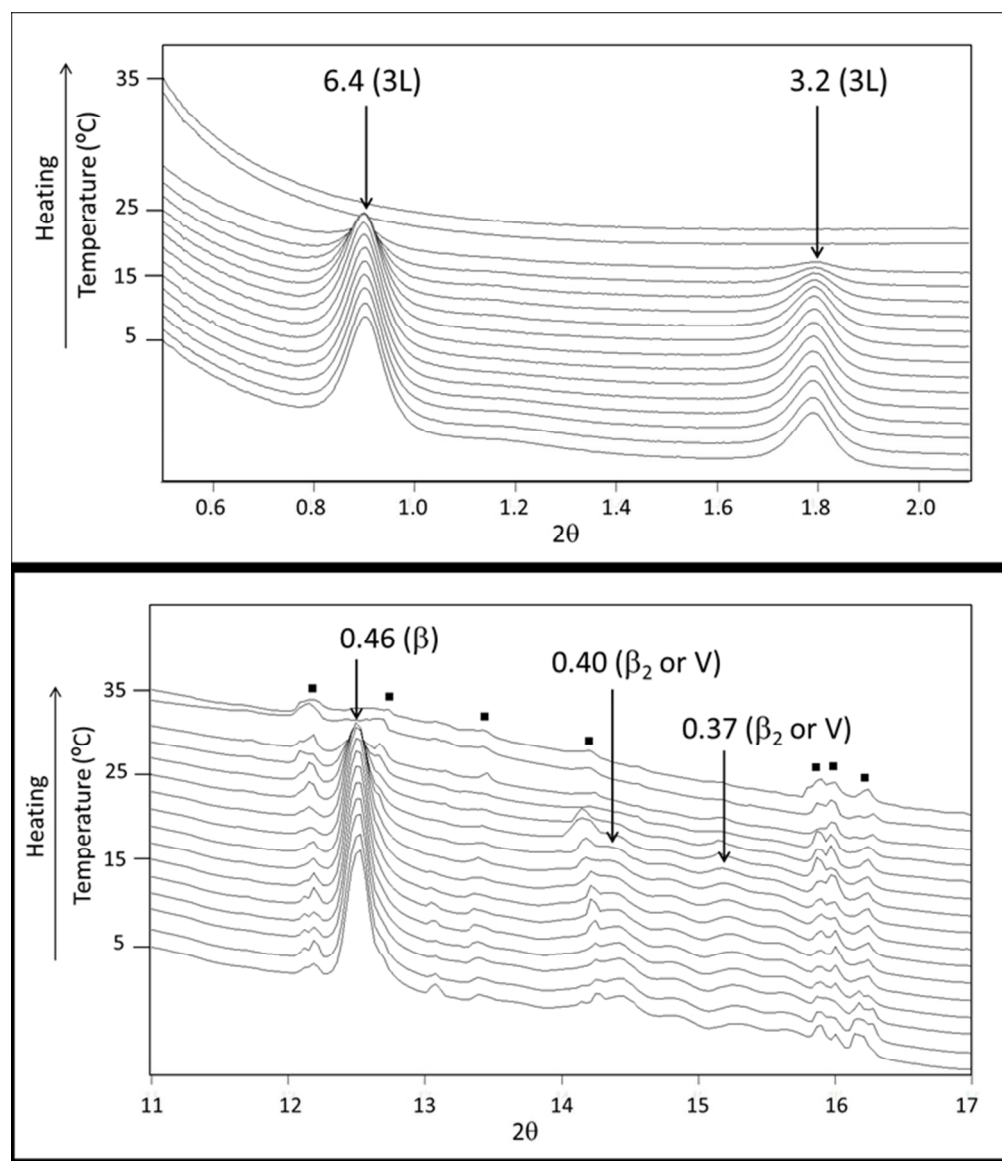




DSC melting curves of velvet and normal chocolate when heated from 5 to 50°C at 2°C/min.  
252x153mm (150 x 150 DPI)

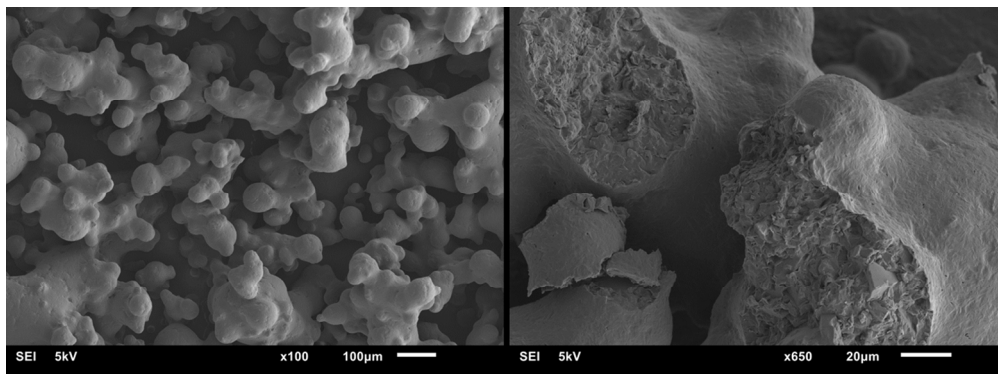


Laboratory-scale XRD of velvet and normal chocolate samples taken at room temperature.  
238x139mm (150 x 150 DPI)

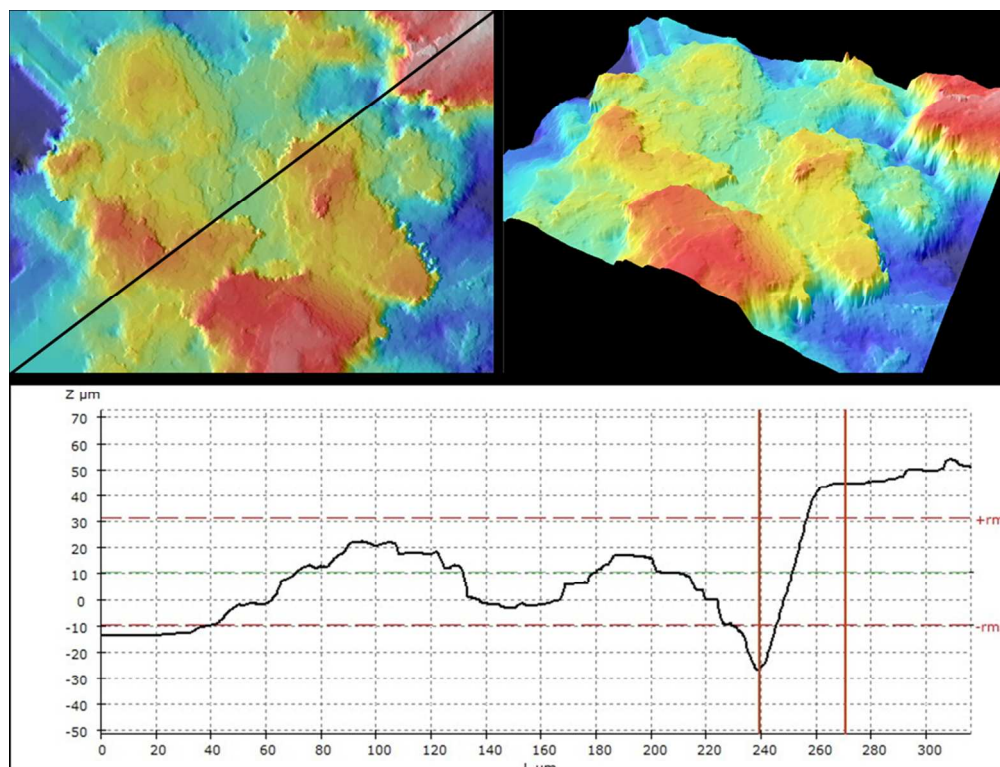


SR-SAXD (up) and SR-WAXD (bottom) patterns of velvet chocolate when heated from 5°C to 40°C at 2°C/min.  
129x149mm (150 x 150 DPI)

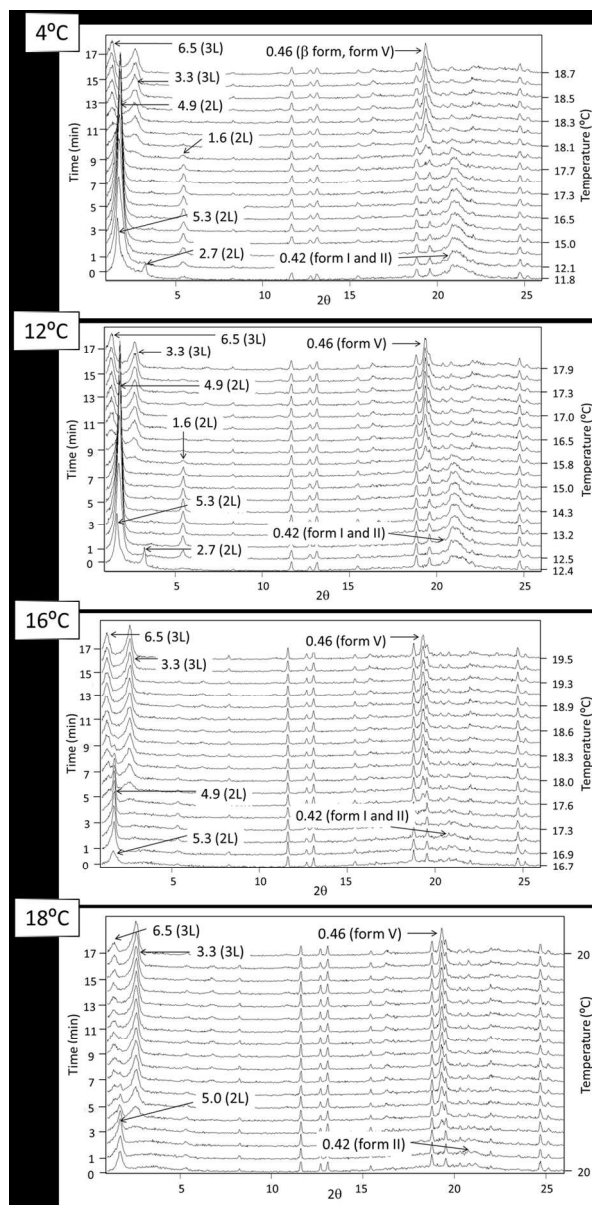
1  
2  
3  
4  
5  
6  
7  
8  
9  
10  
11  
12  
13  
14  
15  
16  
17  
18  
19  
20  
21  
22  
23  
24  
25  
26  
27  
28  
29  
30  
31  
32  
33  
34  
35  
36  
37  
38  
39  
40  
41  
42  
43  
44  
45  
46  
47  
48  
49  
50  
51  
52  
53  
54  
55  
56  
57  
58  
59  
60



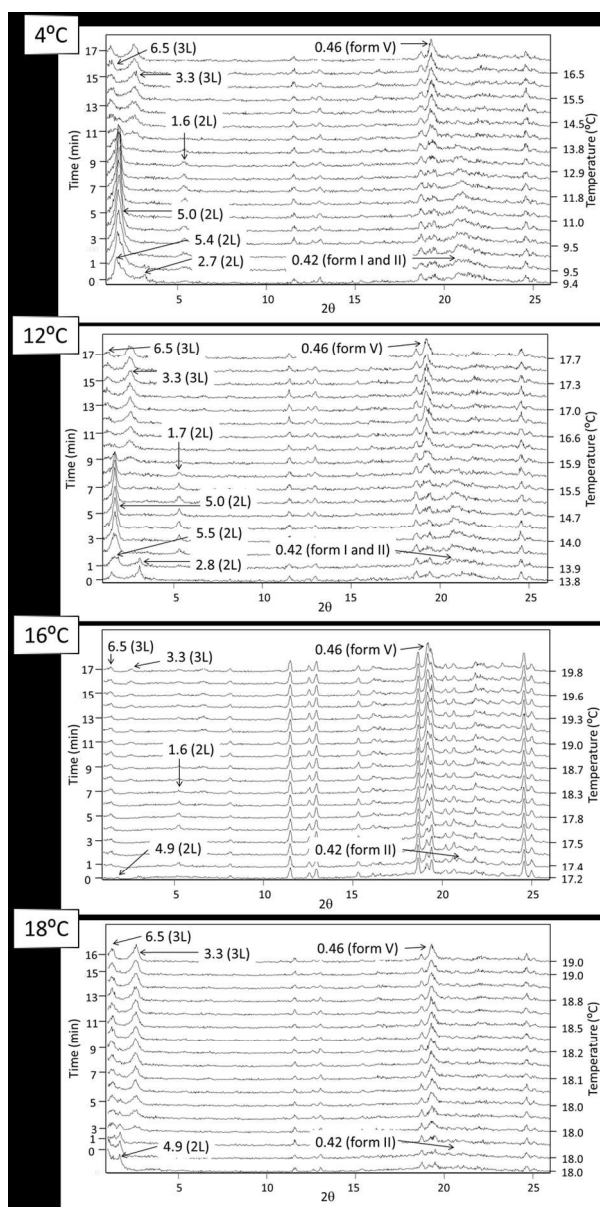
Cryo-SEM images of velvet chocolate  
236x88mm (150 x 150 DPI)



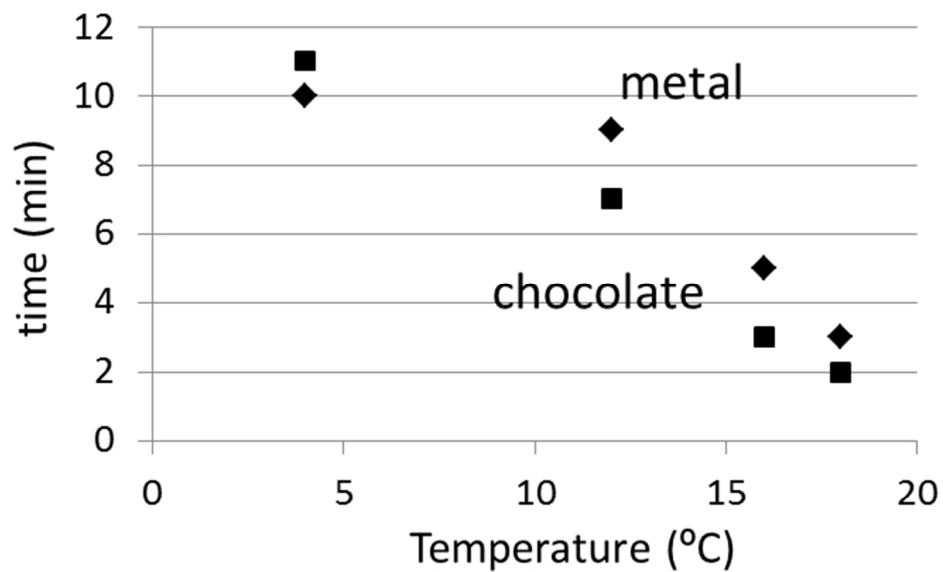
Confocal interferometric scanning microscopy image in 2D (top-left) and 3D (top-right), and profile of peak-to-valley heights (bottom). The profile depicted corresponds to the direction noted by a line in the 2D image.  
182x138mm (150 x 150 DPI)



Laboratory-scale XRD patterns obtained when fluidized chocolate was sprayed on metal substrate at 4, 12, 16 and 18°C, and heated to room temperature.  
163x330mm (150 x 150 DPI)



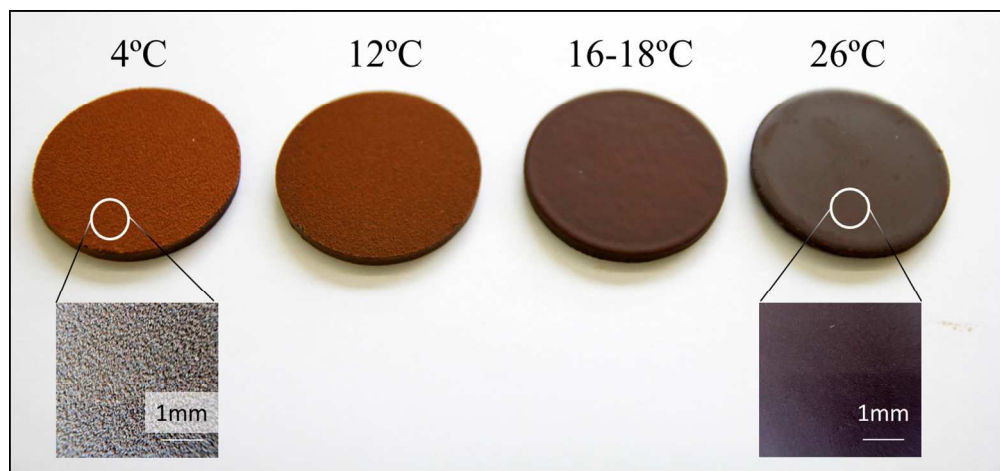
Laboratory-scale XRD patterns obtained when fluidized chocolate was sprayed on chocolate substrate at 4, 12, 16 and 18°C, and heated to room temperature.  
164x328mm (150 x 150 DPI)



Duration for form V formation of CB crystals on metal and chocolate substrates at the different temperatures.

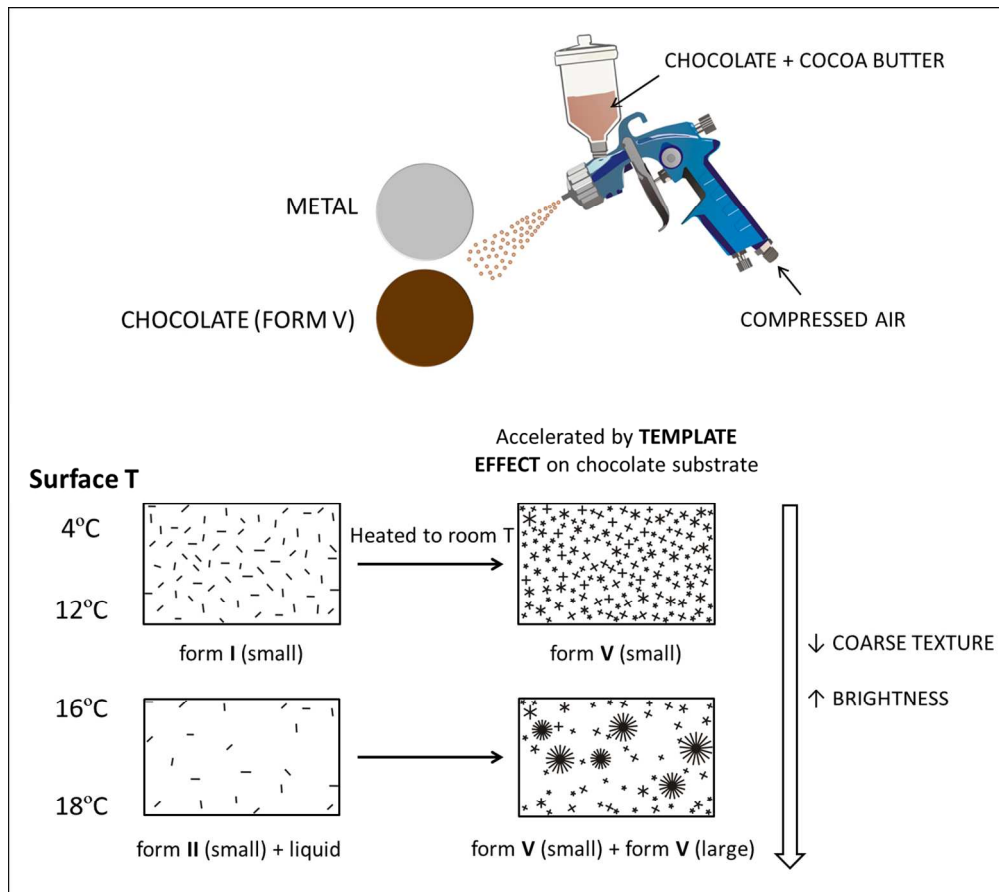
120x77mm (150 x 150 DPI)





Appearance of velvet grown on chocolate surface at 4, 12, 16-18 and 26°C.  
255x118mm (150 x 150 DPI)

1  
2  
3  
4  
5  
6  
7  
8  
9  
10  
11  
12  
13  
14  
15  
16  
17  
18  
19  
20  
21  
22  
23  
24  
25  
26  
27  
28  
29  
30  
31  
32  
33  
34  
35  
36  
37  
38  
39  
40  
41  
42  
43  
44  
45  
46  
47  
48  
49  
50  
51  
52  
53  
54  
55  
56  
57  
58  
59  
60



Models for describing the microstructure of velvet chocolate when grown at different surface temperatures on chocolate substrate.  
245x218mm (150 x 150 DPI)